Published online 26 August 2006 *Nucleic Acids Research, 2006, Vol. 34, No. 16* ***4375–4386***
doi:10.1093/nar/gkl558

Apoptosis resistance downstream of eIF4E: posttranscriptional activation of an anti-apoptotic transcript carrying a consensus hairpin structure

Ola Larsson*, David M. Perlman, Danhua Fan, Cavan S. Reilly[1], Mark Peterson, Cecilia Dahlgren[2], Zicai Liang[2], Shunan Li, Vitaly A. Polunovsky, Claes Wahlestedt[3] and Peter B. Bitterman*

Department of Medicine, University of Minnesota, MMC 276, USA, [1]School of Public Health Division of Biostatistics, University of Minnesota, Minneapolis, MN 55455, USA, [2]Department of Cell and Molecular Biology (CMB), Programme for Genomics and Bioinformatics, Karolinska Institutet, Berzelius väg 35, 171 77 Stockholm, Sweden and [3]Scripps Florida, 5353 Parkside Drive, RF2, Jupiter, FL 33458, USA

Received April 25, 2006; Revised July 7, 2006; Accepted July 18, 2006 Gene expression Omnibus accession no. GSE 2094

ABSTRACT

Aberrant activation of the translation initiation machinery is a common property of malignant cells, and is essential for breast carcinoma cells to manifest a malignant phenotype. How does sustained activation of the rate limiting step in protein synthesis so fundamentally alter a cell? In this report, we test the post transcriptional operon theory as a possible mechanism, employing a model system in which apoptosis resistance is conferred on NIH 3T3 cells by ectopic expression of eIF4E. We show (i) there is a set of 255 transcripts that manifest an increase in translational efficiency during eIF4E-mediated escape from apoptosis; (ii) there is a novel prototype 55 nt RNA consensus hairpin structure that is overrepresented in the 5′-untranslated region of translationally activated transcripts; (iii) the identified consensus hairpin structure is sufficient to target a reporter mRNA for translational activation under pro-apoptotic stress, but only when eIF4E is deregulated; and (iv) that osteopontin, one of the translationally activated transcripts harboring the identified consensus hairpin structure functions as one mediator of the apoptosis resistance seen in our model. Our findings offer genome-wide insights into the mechanism of eIF4E-mediated apoptosis resistance and provide a paradigm for the systematic study of posttranscriptional control in normal biology and disease.

INTRODUCTION

The posttranscriptional operon theory suggests that genes are co-regulated at the level of mRNA splicing, export, localization, translational efficiency and stability—resulting in a posttranscriptional control step for each individual transcript based on sequence information in the RNA (1). As a result, posttranscriptional control represents the critical nexus linking the transcriptome to the proteome. Posttranscriptional control is used by the cell to regulate critical life cycle events including differentiation, cell cycle transit and apoptosis (2–4). Previously examined in the context of normal cellular processes (5), derangements of posttranscriptional control are now being identified in a number of pathological states including cancer (6–8), cardiovascular disorders (9,10) and obesity (11).

More than a decade of research has connected pathological changes in the translational machinery to a number of human malignancies including breast cancer, head and neck squamous cell carcinoma, and cancer of the prostate (12). In cancer, the most frequently documented aberrancy in the translational apparatus is overexpression of eukaryotic translation initiation factor 4E (eIF4E), which selectively affects transport of specific transcripts (13), increases cap-dependent translation, suppresses apoptosis and leads to malignant transformation (14,15). In this regard, we have found recently that pathological activation of the translation initiation apparatus is not simply a secondary consequence of the intrinsic need of human cancer cells for increased protein synthesis, but rather is essential for expression of a transformed phenotype (16).

An invariant property of malignant cells is the ability to evade apoptosis. A large repertoire of physiological

*To whom correspondence should be addressed. Tel: +1 612 626 6848; Fax: +1 612 625 2174; Email: larss004@tc.umn.edu
*Correspondence may also be addressed to Peter Bitterman. Tel: +1 612 624 5175; Fax: +1 612 625 2174; Email: bitte001@umn.edu

The authors wish it to be known that, in their opinion, the second and third authors should be regarded as joint Second Authors

regulatory cues antagonizing apoptosis activate eIF4E by signaling through the Akt-mediated kinase cascade; and recent work has directly traced the anti-apoptotic and oncogenic function of Akt to eIF4E, identifying the translation initiation apparatus as a point of convergence and integration of potentially oncogenic signals (17). Although a few of the transcripts mediating the pro-neoplastic function of eIF4E have been deduced and validated (12,18), a genome-wide analysis of the transcripts utilized by activated eIF4E to interdict apoptosis and produce a neoplastic phenotype has not been reported.

If rescue from apoptosis by eIF4E occurs through the active recruitment of ribosomes to certain transcripts and not to others, then elucidating the rules governing this process become an important goal. The posttranscriptional operon model posited by Keene and Lager (1) suggests that by recognizing related combinations of sequence element in the 5′- and 3′-UTRs (5′- and 3′-untranslated regions) of transcripts, higher eukaryotes can co-regulate translation of mRNA subsets with a shared physiological function. Thus, by identifying genes that are translationally co-regulated by a cell under a given condition, it may be possible to identify new putative mRNA sequence elements mediating the co-regulation. There is support for the hypothesis of co-regulation dictated by RNA elements, as elements mediating specific binding to the Puf proteins have been described recently in yeast (19). Most of the currently recognized translational regulatory elements are found in the untranslated regions of transcripts, and all known mRNA regulatory elements have been collected in the UTRsite database (20).

We sought to identify those transcripts functioning in the downstream mechanism of eIF4E-mediated apoptosis resistance by combining estimates of mRNA translational efficiency and abundance to identify shared nucleotide sequences in the identified transcripts that might mediate the co-regulation, and to inform functional studies using RNA interference. The approach stratifies the mRNA population of a cell based on translational activity using polyribosome preparations, a well-defined procedure for separating transcripts based on the number of ribosomes each transcript has bound (21), and probes the stratified transcripts with microarrays. Our global analysis of gene expression represents an advance over prior studies of posttranscriptional control in which RNA from polyribosome preparations has been used to study recruitment of ribosomes to individual transcripts of interest using northern blotting or real-time PCR (RT–PCR) (18,21). In addition, although prior studies have addressed the downstream effects of activating eIF4E using polyribosome preparations in combination with microarrays; they have used rapamycin as a tool to inactivate eIF4E—an approach that also alters other key cellular functions including ribosomal biogenesis (22,23) and have not systematically addressed the mechanism of eIF4E-mediated apoptotic rescue.

Here we report a genome-wide analysis of transcripts that are translationally activated when cells are rescued from a pro-apoptotic stress by overexpression of eIF4E. Our study includes a systematic UTR search identifying a consensus hairpin structure that mediates translational activation specifically under pro-apoptotic conditions, as well as siRNA-mediated knockdown experiments to assess the functional import of one prototype transcript harboring the regulatory consensus hairpin structure, osteopontin.

MATERIALS AND METHODS

Cell lines and culture

NIH 3T3 cells and NIH 3T3 cells ectopically expressing eIF4E (which are apoptosis resistant and tumorigenic) have been described previously (15).

Apoptosis induction

Two different stimuli were used to induce apoptosis. Cells were either serum starved in DMEM + 0.1% fetal bovine serum (FBS) for 16 h to trigger intrinsic apoptosis, or treated with the calcium ionophore A23187 at 5 μM for 6 h as an endoplasmic reticulum stressor.

RNA preparation and fractionation

Poly(A) RNA: NIH 3T3 cells cultured in standard media (DMEM + 10% FBS) were lysed, and poly(A) RNA was isolated using the PolyATract System 1000 kit (Promega) according to the manufacturer's protocol.

Polyribosome RNA: Polyribosome stratified RNA was fractionated and prepared as described previously (18,21). For microarray samples, 10 fractions of 0.5 ml were collected into tubes containing 50 μl of 10% SDS. RNA in the fractions was purified using Tri-reagent (Sigma), fractions 4–6 were combined into the 'light' fraction, and fractions 7–10 were combined into the 'heavy' fraction. Although fractions 1–3 were of interest, RNA quantity and purity was insufficient for reproducible analysis.

cDNA labeling and hybridization

Fractionated RNA (10 μg) or NIH 3T3 poly(A) RNA (1 μg) was labeled using the Cyscribe kit (Amersham Pharmacia Biotech). The samples were washed using a QIAquick PCR purification kit (Qiagen) with an extended washing procedure (total of four rounds of washing) and vacuum dried. The samples were hybridized onto pre-hybridized [45 min at 42°C in 5× SSC, 5× Denhardts solution (Amersham Pharmacia Biotech), 0.02 μg/μl tRNA (Life Technologies), 0.5% SDS and 50% formamide (Sigma)] Toronto 15k mouse chips (Ontario Cancer Institute) using the Cyscribe hybridization buffer, including cot-1 DNA (10 μg) (Life Technologies), tRNA (20 μg) (Life Technologies) and oligo pd(A) (1 μg; Amersham Pharmacia Biotech) at 42°C for 16 h according to the Cyscribe kit instructions. After hybridization, the chips were washed and scanned (Hewlet Packard Scan Array 5000).

Image and data analysis

All experiments were performed in biological duplicates including polyribosome preparations except for the ionophore set where one pilot chip was run to help prioritize the data from the serum stress studies. Each gene/EST was spotted in duplicate on both microarrays used (see below). Images of similar quality from each chip were digitized using Scan Array 5000 (Hewlett Packard).

We used a combination of fold change and a statistical test called 'Significance analysis of microarrays' (SAM) (24) and applied it as described previously (25). SAM is a non-parametric test that uses the variation in the dataset to calculate the significance (the false discovery rate, FDR). The candidate genes were selected by first identifying all genes for which NIH 3T3/4E-Heavy-apoptogenic/NIH 3T3-Heavy-apoptogenic > 2 and NIH 3T3/4E-Heavy-apoptogenic ≠ NIH 3T3-Heavy-apoptogenic (SAM FDR < 0.05). This set of genes was further categorized as follows [grouping strategies have been used previously in cell fate studies to increase biological coherence within each sub-group (26)]:

Group 1: NIH 3T3-Heavy-basal/NIH 3T3-Heavy-apoptogenic > 2 and NIH 3T3-Heavy-basal ≠ NIH 3T3-Heavy-apoptogenic (SAM FDR < 0.05).

Group 2: NIH 3T3/4E-Heavy-apoptogenic/NIH 3T3/4E-Heavy-basal > 2 and NIH 3T3/4E-Heavy-apoptogenic ≠ NIH 3T3/4E-Heavy-basal (SAM FDR < 0.05).

Group 3: Neither group 1 nor 2.

If a gene represented by several different ESTs/cDNAs on the Ontario array appeared in several groups, (2% of the total) the gene was assigned to the group where the majority of cDNAs/ESTs were assigned. Some genes passed criteria for group 2 as well as criteria for either group 1 or group 3. When this occurred, the genes were assigned to group 2 (3% of the total), as this indicates that the gene is potentially of greater biological significance.

Real-time PCR

The RNA samples were treated with DNAse (Turbo DNase; Ambion) and converted to cDNA using the TaqMan reverse transriptase kit (Roche). Real-time PCR was performed using the Roche Light-Cycler with SYBR Green dye (Roche). The primers were Spp1 5′-AAATTATTGGTGACTTGGTGGTGA and 5′-CTGTAGGGACGATTGGAGTGAAA; Fah 5′-TGCCCTCATGCCCTTTGTGGTG and 5′-CCGCCTGGCTCATTCCTTCTCC; Gsta4 5′-ACCCCCAAGGAAAAAGAGGAGAGC and GGCATTTGTCATTGTGGGCAGAGT; EIF4E 5′-AACAAGCAGCAGAGACGGAGTGAC and 5′-TTGGGGGTGGGGGAGGAG; Arpc1a 5′-caggctcctgtgacttcaaat and 5′-tggcttctcatccacctctt; Cyc1 5′-acctggtgggagtgtgctac and 5′-catcctggacctccacctc; pGL3 luciferase 5′-tgagtacttcgaaatgtccgttc and 5′-gtattcagcccatatcgtttcat. All PCRs were subsequently subjected to gel electrophoresis to confirm the presence of a single PCR product of the appropriate length.

Western blotting

Western blotting was performed as described previously (16) using an anti-mouse osteopontin antibody (R&D Systems Inc., Minneapolis MN) at 1:1000 dilution.

siRNA experiments

NIH 3T3/4E cells in mid log phase growth were transfected with siRNA using Lipofectamine 2000 in Opti-MEM (Life Technologies, according to the manufacturer's directions) for 4 h, allowed to recover for 20 h in complete media, then shifted to DMEM supplemented with 0.1% FBS as the apoptogenic stress or allowed to continue in complete media for the time indicated. The siRNAs were osteopontin siRNA#1 GACATCAACTGTGCCTCATdTdT and osteopontin siRNA#2 GAGGUAGAAAAGGCACACATTdTdT. A scrambled osteopontin siRNA#1 GACAGCGTTGAATCCTCATdTdT was used as control. Parallel experiments using pEGFP-N3 (carrying GFP) resulted in an estimated transfection efficiency in the range of 90%.

FACS analysis

Frequency of apoptosis was quantified by flow cytometric analysis of the percentage of cells with hypodiploid DNA content as described previously using standard optics of the FACScan flow cytometer (Becton Dickinson) and the CellQuest Pro program.

Searching mRNA sequence elements

Full-length mRNA sequences of corresponding EST sequences from the Toronto microarray chips were extracted from mouse RefSeq mRNAs listed as of October 2004. These full-length sequence files were loaded into UTRscan software to identify mRNA sequence elements that were collected in the UTRsite database at URL http://www.ba.itb.cnr.it/BIG/UTRScan/.

Fisher's exact test

Fisher's exact tests were performed in R (R-project.org) to determine whether the percentages of sequences containing each mRNA element were different when groups 1, 2 and 3 (as described in Image and data analysis) were compared individually to random control transcripts, which contained 251 RefSeq mRNA sequences corresponding to EST sequences randomly selected from the Toronto microarray gene list.

Searching for novel mRNA elements

Using BioProspector and BioOptimizer (27,28), common mRNA elements were identified in the 5′-UTRs of genes for which (NIH 3T3/4E-Heavy-apoptogenic/NIH 3T3-Heavy-apoptogenic) > 2 and NIH 3T3/4E-Heavy-apoptogenic ≠ NIH 3T3-Heavy-apoptogenic (SAM FDR < 0.05) from a training dataset (the RefSeqs that were used for the analysis are shown in Supplementary Data 1). The training dataset was generated using an earlier chip version and different hybridization conditions, and therefore could not be reliably combined with the rest of the study (i.e. when cells had serum). Therefore, we repeated the initial part of the study (when cells were serum starved) and present these data in the manuscript (Supplementary Table 1). The 5′-UTRs of transcripts in random control transcripts were used as a background. BioProspector and BioOptimizer were used to identify elements ranging from 4 to 50 nt in length with default parameters. The consensus sequences were displayed by WebLogo (http://weblogo.berkeley.edu/). Secondary structure prediction was carried out using RNAfold software at URL (http://rna.tbi.univie.ac.at/cgi-bin/RNAfold.cgi). The genes that carried the consensus hairpin structure from the training dataset as well as those from the final dataset with scores greater than the threshold established in the training dataset are shown (Table 1). For nucleic acid sequence conservation, we identified the human and rat

Table 1. Genes with the identified 55mer 5′-UTR consensus hairpin structure

Gene annotation	Number of copies	RefSeq ID
Mus musculus ornithine decarboxylase, structural 1 (Odc1)	1	NM_013614
M.musculus secreted phosphoprotein 1 (Spp1)	2	NM_009263
M.musculus sex comb on midleg homolog 1 (Scmh1)	2	NM_013883
Homo sapiens regulator of chromosome condensation 2 (RCC2)	1	NM_018715
This record was temporarily removed by RefSeq staff for additional review.	4	NM_138953
M.musculus heterogeneous nuclear ribonucleoprotein C (Hnrpc)	1	NM_016884
M.musculus intracisternal A particles (Iap)	1	NM_010490
M.musculus prune homolog (Drosophila) (Prune)	2	NM_173347
M.musculus nucleosome assembly protein 1-like 1 (Nap1l1)	3	NM_015781
M.musculus ring finger protein (C3H2C3 type) 6 (Rnf6)	1	NM_028774
H.sapiens tankyrase 1 binding protein 1, 182kDa (TNKS1BP1)	2	NM_033396
M.musculus activated leukocyte cell adhesion molecule (Alcam)	5	NM_009655
M.musculus myristoylated alanine rich protein kinase C substrate (Marcks)	1	NM_008538
M.musculus A kinase (PRKA) anchor protein 2 (Akap2)	1	NM_009649

orthologs and searched for the corresponding mouse element in the 5′-UTR using Blast.

Functional studies of novel mRNA elements

The 5′ stem–loop was cloned into both the HindIII (close to the transcription start site) and the NcoI site (close to the translation start site) of the pGL3 control vector from Promega. To generate the HinIII stem, the 'STEM' oligonucleotide (5′-CTAG TCTAGA CTAG TAAAG TGGCG TGTTG AGTTA AATAA AGAGT TTCTT TTTCA AATAT CTAAG GAAAT CTAG TCTAGA CTAG) harboring the stem sequence was primed with CTAG TCTAGA CTAG ATTTC, filled in using Klenow and cloned blunt onto the blunted HinIII site of Luciferase of the pGL3 control vector. To generate the NcoI construct, the 'STEM' oligonucleotide was PCR amplified using primers 5′-CTAG CCATGG CTAG ATTTC CTTAG ATAT and 5′-CTAG CCATGG CTAG TAAAG TGGCG TGTT, cut by NcoI and cloned into the NcoI site of the pGL3 plasmid. Two separate clones from both constructs were sequence validated and used in the dual luciferase assay. For the dual luciferase assay, NIH 3T3 and NIH 3T3/4E cells were seeded in 24-well clusters, and after 24 h cells were transfected with 0.5 μg of the pGL3, pGL3-NcoI-STEM or pGL3-HindIII-STEM (the firefly luciferase plasmid) mixed with 0.05 μg of the pRL-TK (the renilla luciferase plasmid; used as a transfection efficiency control). Transfections were performed for 4 h as described in the section designated 'siRNA experiments'. Immediately after the 4 h transfection, the media was changed to either DMEM with 10% FBS or DMEM with 0.1% FBS. Cells were harvested 16 h after the media change and analyzed using the dual luciferase assay procedure (Promega). The ratios obtained between firefly luciferase (the GL3 derived constructs) and renilla luciferase (pRL-TK) (the ratio controls for transfection efficency) were used to create a ratio between serum starved and serum replete cells. This normalization removed transcriptional/translational effects that differ between the constructs and cell types to enable a clear analysis of the effects of the stem. These ratios were normalized to the ratios obtained for GL3 without the stem–loop within each replicate and the results across replicates were analyzed using *t*-statistics. The experiment was repeated in NIH 3T3/4E cells measuring the mRNA levels of the pGL3 luciferase using the primers described in Real-time PCR above.

Global search for transcripts carrying the 55mer

We generated a scoring matrix using all the identified 55mer elements from the 12 identified transcripts carrying the element and scanned the 5′-UTRs of all mouse transcripts defined in the RefSeq database. All transcripts were ranked based on their score and the top 1000 were used to look for overrepresentation of functions within the selected group of genes as defined by gene ontologies using the EASE tool (29). All RefSeq genes were used as a background. Only categories with more than one hit, showing a relative enrichment of >2 and a Fischer's exact test *P*-value of <0.05 are presented in Supplementary Table 2.

RESULTS

Genome-wide study of apoptotic rescue by eIF4E

To globally address the issue of which transcripts mediate the anti-apoptotic functions of eIF4E, we used a model in which NIH 3T3 cells ectopically overexpress translation initiation factor 4E (eIF4E) resulting in an apoptosis-resistant and tumorigenic phenotype (15). We performed a comprehensive study of apoptosis resistance in the NIH 3T3/4E model using an array containing 15k cDNAs and ESTs (NIH 15k collection printed at The Ontario Cancer Institute). To facilitate data analysis in the two-color competitive hybridization microarray approach employed, we used a universal standard mRNA [non-stratified poly(A) selected RNA derived from NIH 3T3 cells cultured in full growth medium]. We compared signals generated from this standard to both the light (fractions 4–6, <1 ribosome/transcript) and the heavy (fractions 7–10, >1 ribosomes/transcript) polyribosome fractions of RNA from NIH 3T3 and NIH 3T3/4E cells cultured either in complete growth medium or after 16 h of serum starvation (Figure 1A shows a representative polyribosome tracing from each of the four conditions), a time point before any evidence of cytochrome c release from the mitochondria (Figure 1B), a signature step at the apex of the cell death program. We selected the 16 h time point in order to identify genes that might govern the decision to enter the apoptotic pathway, and exclude those involved in the actual process of cell execution.

To be able to distinguish genes that might encode true apoptosis rescue proteins from those that are related to the stimulus applied (serum starvation), we used a second agent,

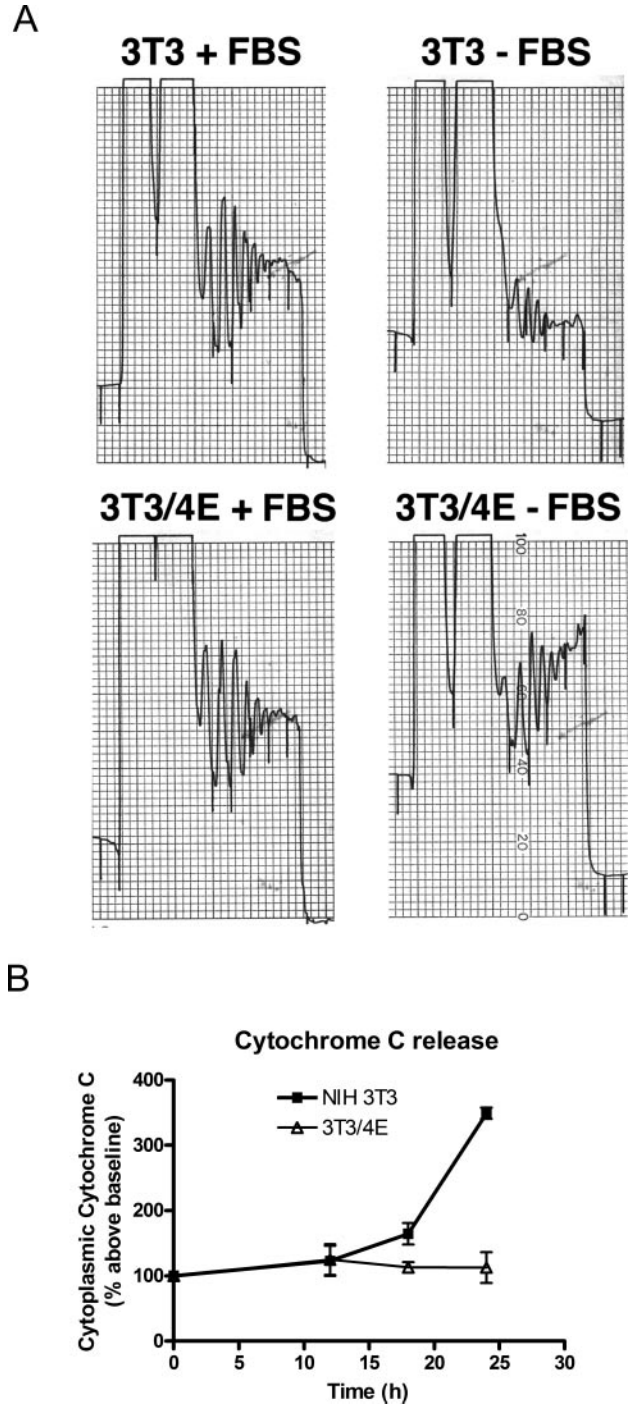

Figure 1. Microarray analysis of polyribosome stratified RNA. (**A**) Polyribosome preparations. Polyribosome preparations were carried out as described previously (18). Shown is the optical density profile (254 nm) of a representative polyribosome preparation for NIH 3T3 and NIH 3T3/4E cells under basal and serum starved conditions. (**B**) Kinetics of mitochondrial release of cytochrome C in serum-starved cells NIH 3T3 and NIH 3T3/4E. Shown is the release of cytochrome c monitored by immunoassay (Quantikine M Rat/Mouse; R&D Systems) as a function of time after shift to serum-free media.

the calcium ionophore A23187 (5 μM), to induce apoptosis. This second apoptogenic stimulus was applied once to aid in parsing our list of candidates to be tested in downstream functional assays. Our rationale was that transcripts experiencing an increase in translational efficiency independent of the apoptotic stimulus are most likely to represent authentic rescue genes.

The data from the serum starvation series were analyzed to identify transcripts that were predominantly present in the heavy fraction of serum-starved NIH 3T3/4E cells compared to serum-starved NIH 3T3 cells (we based our primary data analysis on the H-fractions, since in principle this should include the most biological information). To distinguish gene products classified as translationally activated in NIH 3T3/4E cells because they were being repressed in NIH 3T3 cells triggered to undergo apoptosis (which we viewed as less relevant genes), from those that were actively selected for translation in the NIH 3T3/4E cells (which are the genes of greatest interest), we separated the original gene pool into three groups (Figure 2). The first group contained those gene products that were down-regulated in NIH 3T3 cells due to serum starvation or activation of the apoptotic program, and therefore only appeared to be up-regulated in NIH 3T3/4E cells. In contrast, the second group contained gene products that were translationally active in NIH 3T3/4E cells subjected to a pro-apoptotic stress compared to the basal state, and therefore represented the best apoptosis rescue candidates. The third group contains gene products that were translationally active in NIH 3T3/4E cells in a constitutive manner (i.e. not induced upon serum starvation), and likely includes candidate anti-apoptotic transcripts of interest. However, this group also includes the vast set of transcripts whose translation is activated by the global function of ectopically expressed eIF4E, and therefore are impractical to pursue as candidate genes. The gene products identified as translationally active in each group are presented (Supplementary Table 1) together with their ratios obtained from the calcium ionophore experiment (ratio between apoptogenic heavy fractions of NIH 3T3/4E and NIH 3T3 cells).

As a test of internal consistency, the group assignment of eIF4E was examined. eIF4E is translationally activated in NIH 3T3/4E cells compared to parental NIH 3T3 cells in a constitutive manner—independent of serum status (15), and therefore should be assigned to group 3. Four different cDNAs/ESTs (each in duplicate on each slide) represent eIF4E on the 15k array. In fact, three of the four eIF4E-cDNAs/ESTs were correctly classified in group 3 with gene products that were translationally activated in the NIH 3T3/4E cells, but not selectively activated by the apoptogenic stimulus. The fourth eIF4E cDNA/EST was misclassified in group 2, along with gene products that are selectively activated in NIH 3T3/4E cells when serum starved. For those gene products represented by a single cDNA/EST, this type of error would increase the number of false positive apoptotic rescue candidates. These results indicated that the grouping procedure was reasonable, but not perfect; probably as a result of random variation.

To determine whether our study accurately identified genes that are translationally activated in NIH 3T3/4E cells when subjected to serum withdrawal, we selected several genes for confirmation using an alternative method—choosing three genes from our list to reflect a range of mRNA size, function and signal intensity on the array: glutathione–*S*-transferase alpha 4 subunit (Gsta4), Fumaryl acetoacetate hydrolase (Fah) and eIF4E. As negative controls we selected

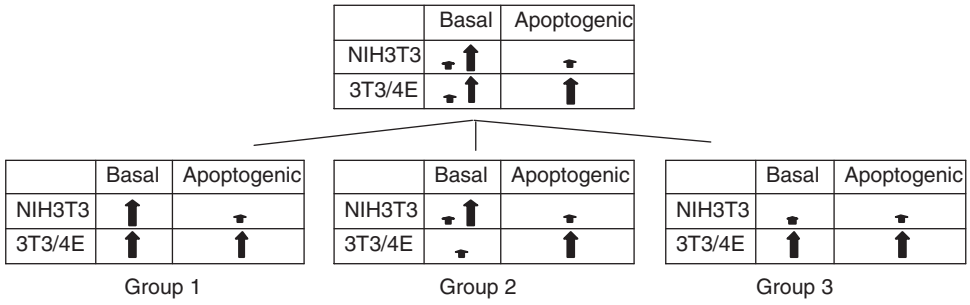

Figure 2. Genome-wide identification of translationally activated transcripts in NIH 3T3 cells rescued from apoptosis by eIF4E. Cells, apoptogenic conditions and procedures for polyribosome and microarray data analysis were as described in Materials and Methods, using the 'Mouse array 15k' from the Micro array center, Ontario Cancer Institute. Shown is a schematic representation of the three groups that resulted from the data analysis approach based on transcript abundance (i.e. signal intensity on the microarray) and statistical significance in the translationally active (heavy) fractions. To simplify presentation, transcript abundance is schematically depicted as arrows of differing sizes. A large arrow designates high abundance, a small arrow designates low abundance, and a large and small arrow together designate either high or low abundance.

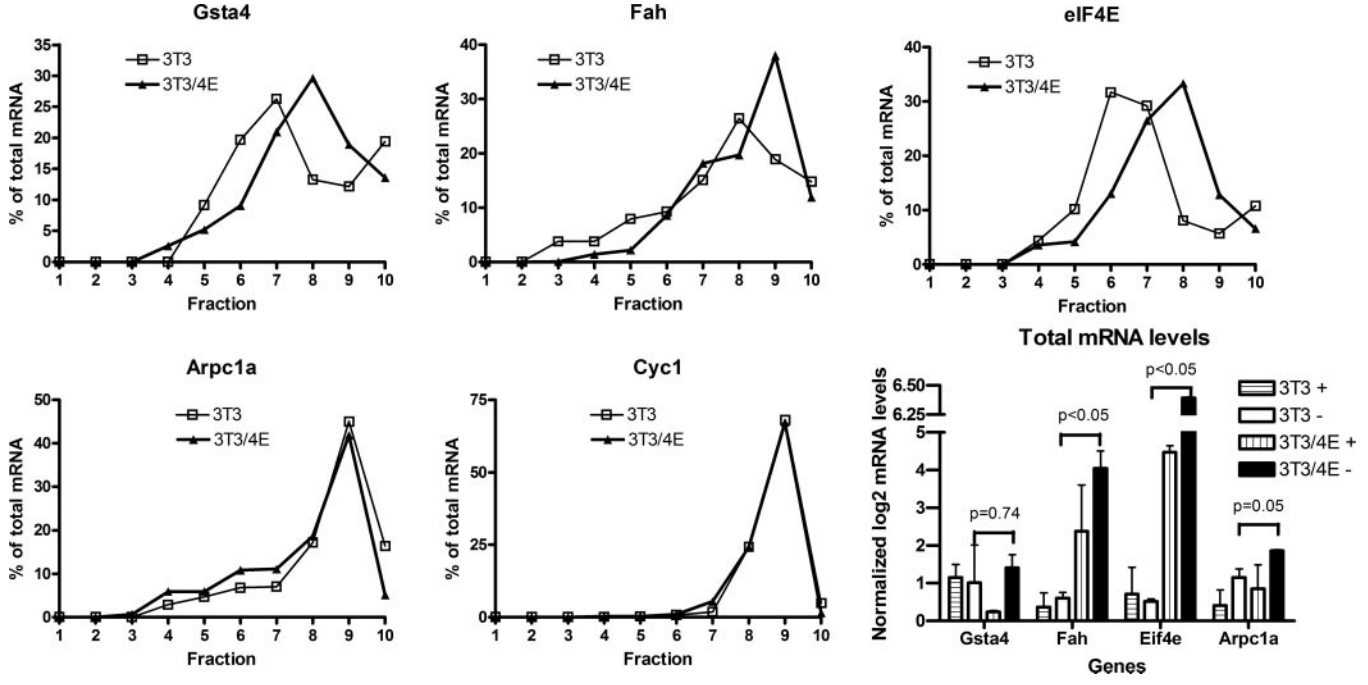

Figure 3. Validation of translational activity. Polyribosomes from NIH 3T3 and NIH 3T3/4E cells subjected to serum withdrawal were separated into 10 size fractions. Three transcripts identified in the array analysis and two transcripts selected as negative controls were analyzed using QRT–PCR across the polyribosome gradient and total mRNA abundance of four of the genes were measured using Cyc1 as an internal control (error bars indicates standard deviations from two independent experiments).

two genes that were easily detected (raw signal >3000 for all measurements), showed no difference between NIH 3T3 and NIH 3T3/4E cells and had a low standard deviation across all measurements: Cytochrome C1 (Cyc1) and Actin related protein 2/3 complex, subunit 1A (Arpc1a). NIH 3T3 and NIH 3T3/4E cells were subjected to serum withdrawal for 16 h, RNA was extracted and stratified by polyribosome size into 10 fractions. Real-time PCR was performed on each of the 10 fractions using primers specific for the selected genes. Each of the three genes selected, but neither of the negative controls, demonstrated a shift from the lighter to heavier (more bound ribosomes) fraction in the NIH 3T3/4E cells compared to the NIH 3T3 cells (Figure 3, the mRNA level has been normalized to show the relative distribution across the fractions for each cell type which is independent of total transcript abundance).

To test whether this translational activation coincided with transcriptional regulation, we also carried out the analysis in NIH 3T3 or NIH 3T3/4E with or without serum using unstratified total RNA. For this analysis, we used Cyc1 as an internal control since it showed remarkably low variation both in our microarray analysis and by confirmatory RT–PCR. As expected, eIF4E was more abundant in the NIH 3T3/4E cells compared to NIH 3T3 cells ($P < 0.05$) independent of serum status, while there was no difference in terms of Gst4a expression between serum stressed NIH 3T3/4E and NIH3T3 cells. Fah ($P < 0.05$) and Arpc1a ($P = 0.05$) (which did not show translational activation) showed

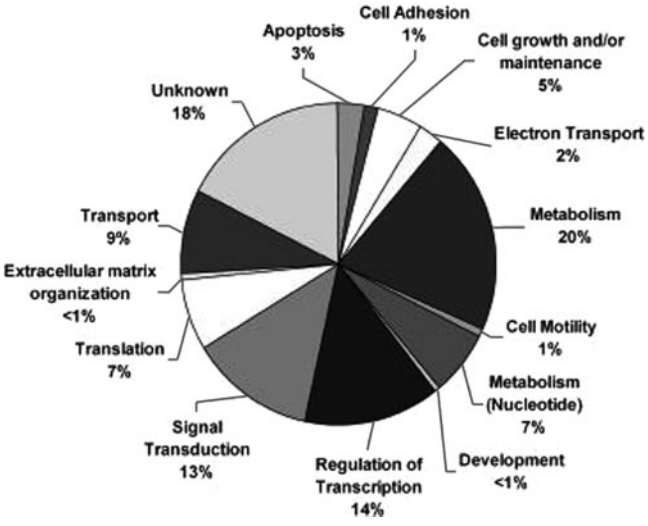

Figure 4. Categorization of translationally activated genes. Genes were categorized using manually curated annotations from the Gene Ontology Consortium (http://www.geneontology.org/). Shown are the percentages of genes from all three groups in each of the functional categories.

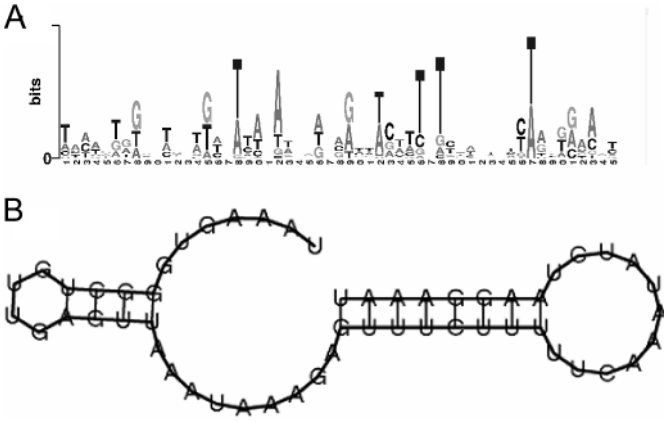

Figure 5. (**A**) A novel mRNA sequence element conserved in the 5′-UTR of transcripts. The sequence was found in the group in which NIH 3T3/4E-Heavy-apoptogenic/NIH 3T3-Heavy-apoptogenic > 2 and NIH 3T3/4E-Heavy-apoptogenic ≠ NIH 3T3-Heavy-apoptogenic (SAM FDR < 0.05). The element was identified by BioProspector and BioOptimizer. The figure shows the bit scores for the four nucleotides at each position of the element as a size shift of the letter symbolizing each nucleotide. (**B**) Structure of the consensus sequence of the 5′ 55mer by RNAfold with default parameters.

increased mRNA levels in NIH 3T3/4E cells compared to NIH 3T3 cells, but only when serum starved. These results indicate that there is no direct relationship between transcriptional activity and translational activity, and suggest that while some genes in our list may be subject to both transcriptional and translational activation, it appears that the procedure employed accurately identifies transcripts experiencing an increase in translational efficiency independent of its abundance. Therefore, our list of genes provides a good starting point to study the mechanisms of translational activation downstream of eIF4E during rescue from apoptosis.

To determine whether certain classes of genes were highly represented among the translationally activated transcripts, we grouped them based on annotations from the Gene Ontology Consortium (GO) (Figure 4, functional assignment is shown in Supplementary Table 1). GO annotation can be non-reliable. We therefore, examined primary literature sources and performed a manual correction. Group 1 contained two transcripts encoding transcription factors and three encoding ribosomal proteins. In group 2, there were many transcripts encoding mitochondrial proteins (15 transcripts). There were also several mRNAs associated with protein kinase activity (11 transcripts) and 19 encoding transcripts involved in the regulation of transcription. Group 3 contained transcripts encoding cell adhesion proteins (two proteins); mitochondrial proteins (six proteins); proteins related to protein biosynthesis either as components of the translation machinery (four proteins) or tRNA synthesis (two proteins); transcription factors (eight proteins); and notably two proteins with glutathione transferase activity—one of which was the most highly activated transcript of all (GSTA4)—a mitochondrial protein that participates in lipid peroxidation. In the aggregate, transcripts associated with transcriptional control, signal transduction, mitochondrial function and the translational machinery itself accounted for about one-third of the translationally activated transcripts.

A novel prototype mRNA consensus hairpin structure targets mRNAs for translational activation by eIF4E

Sequence elements in mRNA have important roles in the posttranscriptional control, especially those residing in the 3′-UTR and 5′-UTR (30). To gain insight into the mechanisms leading to the translational activation of genes which were translationally activated by ectopic eIF4E expression in the context of rescue from apoptosis, we sought to identify shared elements in either the 3′- or 5′-UTR. When full-length sequence files were loaded into UTRscan software to identify mRNA sequence elements represented in the UTRsite database, none of the elements showed a statistically significant association with group assignment (groups 1–3 or when groups 1–3 were pooled). Thus known RNA regulatory elements could not account for the observed translational activation. Recently, a 3′-UTR element was identified to be responsible for transport of cyclin D1 from the nucleus to the cytoplasm (31). This element is not included in the UTRSite, so we manually tested for its occurrence. When using BLAST to identify similar sequences to the mouse sequence reported in the study (31), we did not identify any significant alignment to any other mouse mRNA (in the RefSeq database). We therefore concluded that this element probably represents a highly mRNA-specific mechanism.

We next sought to computationally identify novel common mRNA sequence elements in the 5′-UTR of those transcripts which were translationally activated in NIH 3T3/4E cells subjected to an apoptogenic stress. For this purpose, we used genes from a training dataset (genes used as input in Supplementary Data 1; Materials and Methods). We utilized BioProspector with default parameters, and the 5′-UTR of random control transcripts served as the background. The output was optimized using BioOptimizer. In the 5′-UTR, the consensus sequence with the highest score was a 55mer (Figure 5A) with a predicted secondary structure (RNAfold) showing two stem–loops (Figure 5B). The minimum free

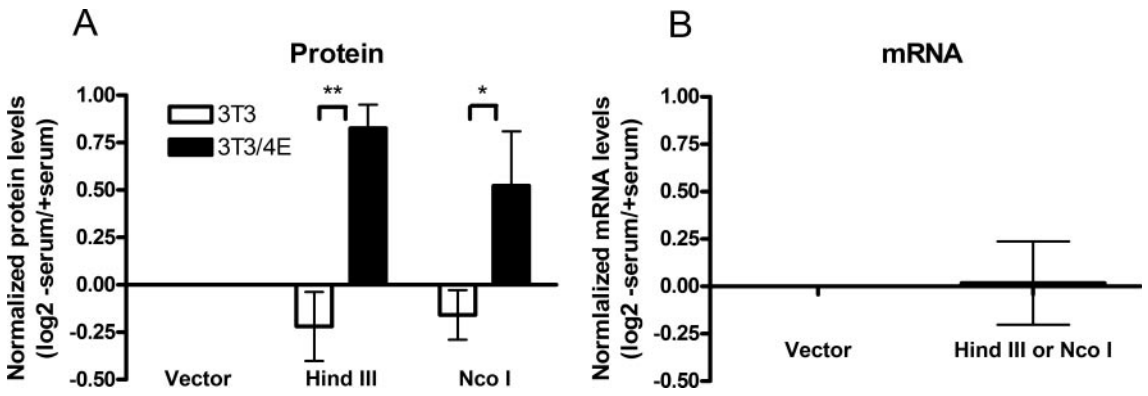

Figure 6. Translational activation mediated by the 55mer 5′-UTR structure. (**A**) Plasmids carrying the 55mer (with bases 9–10 flipped to avoid a cryptic translational start site as these positions were essentially not conserved at all across the 14 genes, Figure 5A bases 9–10) at two different positions (the HindIII positions the 55mer close to the transcription start site whereas the NcoI positions the 55mer close to the translational start site with a distance of ∼30 nt from the two sites) were transfected into NIH 3T3 and NIH 3T3/4E cells, which were serum starved or maintained in normal media. The cells were harvested after 16 h and relative protein levels were measured using the dual luciferase assay. Shown are the ratios between serum starved and serum replete cells. Each experiment was normalized to the basic vector pGL3 control and the experiment was repeated three times in duplicate (two different constructs showed similar results and were pooled). (Error bars indicate standard deviation, *students *t*-test *P*-value <0.05 and **students *t*-test *P*-value <0.001.) (**B**) The experiment was repeated in NIH 3T3/4E cells while measuring the mRNA level of the luciferase-gene carrying the 55mer. The data were normalized as in Figure 6A. (Error bars indicate standard deviations from three to four independent measurements, pooled from the two constructs.)

energy of this structure is −6.50 kcal/mol. A total of 14 transcripts, from either the training dataset or the final dataset, presented in Table 1, were predicted to contain this consensus sequence, with each transcript containing between 1 and 5 copies. Of 27 identified elements 26 folded into various hairpin-like structures (Supplementary Figure 1). To test whether the nucleic acid sequence of the hairpin structure was conserved, we looked for conservation across human, mouse and rat, and identified conservation of the entire element in three elements and partial conservation in two but only between two species. This shows that the 55mer is not highly conserved based on sequence (Supplementary Data 2). Together, these findings indicate that we have identified a hairpin structure with consensus characteristics. We therefore use the term consensus hairpin structure to characterize the element. It should be noted that ornithine decarboxylase (ODC), one of the first transcripts documented to experience a selective increase in translational efficiency when eIF4E is overexpressed (21), harbors the consensus hairpin structure.

To assess whether the identified 5′ consensus hairpin structure could mediate translational activation in response to eIF4E, we cloned the consensus sequence for the 55mer (with bases 9–10 flipped to avoid a cryptic translational start site as these positions were not conserved, see Figure 5A bases 9–10) into the 5′-UTR of luciferase at two different positions and used the dual luciferase assay to quantify protein and mRNA levels in both NIH 3T3 and NIH 3T3/4E cells under serum replete or serum restricted conditions (Figure 6). Insertion of the consensus hairpin structure into the 5′-UTR mediated a relative increased protein activity (Figure 6A). The effect of the 5′-UTR consensus hairpin structure was independent of position within the luciferase 5′-UTR. To determine whether these changes in protein levels were independent of changes in mRNA levels, we measured the expression of the luciferase transcript in NIH 3T3/4E cells using RT–PCR. As our protein experiments indicated no difference between the two luciferase constructs carrying the 55mer, the data from these were pooled. There were no changes in mRNA levels that could explain the changes in protein activity observed (Figure 6B).

To test the hypothesis that transcripts serving a common cellular function share sequence elements that could enable groups of genes with similar functions to be co-regulated downstream of eIF4E, we used a bioinformatic approach. Finding such a structure–function correlation would indicate that groups of genes with similar functions could be regulated by structural features in their UTRs downstream of eIF4E. This would, together with the identification of the consensus hairpin structure from our set of deregulated genes, indicate that this is one of the mechanisms by which eIF4E could carry out its pleotropic functions. To see if the consensus hairpin structure could be associated with certain categories of genes as described by the GO Consortium (32,33), we scanned the 5′-UTRs of all mouse mRNA defined in the RefSeq database for the presence of the 55mer and looked for overrepresentation of GO categories (29). This provided a ranking of all RefSeq mRNAs based on having a sequence close to the consensus sequence. Although in principle this provisional list should be enriched for genes having the consensus hairpin structure, it will also include many that may not. When using the top 1000 genes containing the 55mer, we identified an overrepresentation of genes relating to apoptosis inhibition, proliferation and differentiation (Supplementary Table 2). This indicates that the consensus hairpin structure identifies groups of transcripts with related functions, and hence provides insights into the mechanisms downstream of deregulated eIF4E (the named genes from the top 300 genes carrying the element are shown in Supplementary Table 3). Thus, as a test of the posttranscriptional operon theory for the mechanisms of deregulated eIF4E, we have identified a consensus hairpin structure that can target transcripts for translational activation during serum starvation only in the context of deregulated eIF4E, and shows that transcripts harboring the 55mer belong to biologically sound, functionally defined classes that could plausibly be co-regulated.

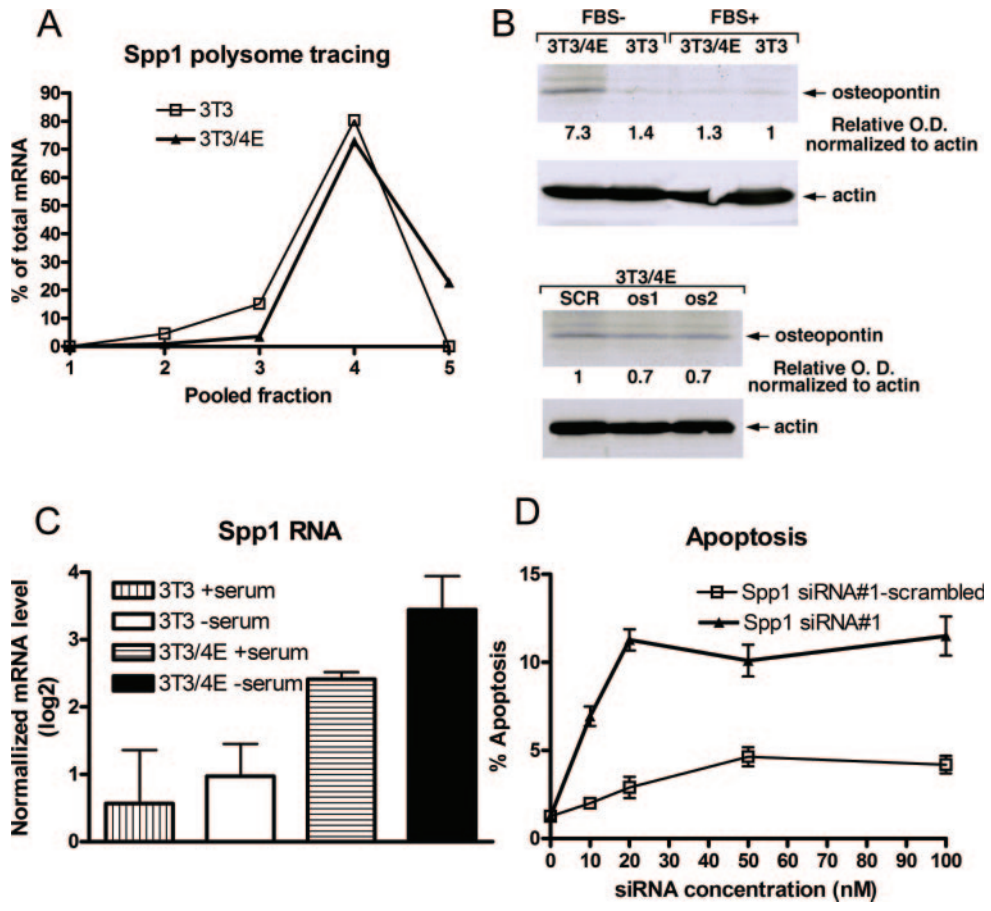

Figure 7. Validation of osteopontin (Spp1) as a translationally activated antagonist of apoptosis. (**A**) RT–PCR quantification of the osteopontin transcript across the polyribosome gradient. Adjacent polyribosome fractions were paired, and osteopontin transcript was quantified by RT–PCR. (**B**) Representative experiment showing osteopontin protein levels in NIH 3T3 and NIH 3T3/4E cells after 16 h serum starvation (upper panel); and osteopontin levels in NIH 3T3/4E cells 48 h after transfection with osteopontin siRNA#1-scrambled (SCR), osteopontin siRNA#1 (os1) and osteopontin siRNA#2 (os2) at 20 nM. (**C**) Osteopontin total mRNA levels in NIH 3T3 and NIH 3T3/4E cells in complete (serum +) and media lacking serum (serum −). (Error bars indicate standard deviation from two independent measurements.) (**D**) Apoptotic frequency of NIH 3T3/4E cells 48 h after serum withdrawal in response to osteopontin (Spp1) siRNA#1 or osteopontin (Spp1) siRNA#1-scrambled siRNA. (Error bars indicate standard deviation from two independent experiments.)

Osteopontin is a translationally activated mediator of apoptosis resistance

Although we predict that our list would be enriched in genes mediating apoptosis resistance, we expect that many contribute to other parts of the pleotropic effects downstream of eIF4E. This notion is supported by the data indicating that apoptosis resistance was not the only abundant GO term identified among transcripts carrying the 55mer. We also found genes e.g. relating to proliferation—another phenotypic characteristic of cells with deregulated eIF4E. When we reviewed those genes carrying the 55mer consensus hairpin structure we found one gene, osteopontin (Spp1), that carried two copies of the 55mer consensus hairpin structure in its 5′-UTR (Table 1) and demonstrated an increase in translational efficiency under both serum starvation and calcium ionophore treatment (Supplementary Table 1). We therefore thought that osteopontin would provide a good test of the hypothesis that genes carrying the functionally defined consensus hairpin structure in their UTRs also mediate the phenotypic effects of deregulated eIF4E, in this case apoptosis resistance. Osteopontin is a growth and survival signal for endothelial cells, smooth muscle cells and melanocytes (34–36). To validate translational activation of osteopontin in our model, we used RT–PCR analysis across the polyribosome gradient. Indeed, we found that osteopontin was translationally activated in NIH 3T3/4E cells compared to control NIH 3T3 cells (Figure 7A, in this tracings fractions were pooled two and two starting from fraction 1) as ∼20% of the mRNA was present in the heaviest polyribosomes of NIH 3T3/4E cells whereas NIH 3T3 cells lacked mRNA in the heaviest polyribosomes. To verify that the shift in translational activation results in increased protein levels, we performed western blotting. Indeed, after 16 h of serum starvation, osteopontin protein expression is increased ∼7-fold in NIH 3T3/4E cells compared to the parental NIH 3T3 cells in complete media (Figure 7B), and ∼6-fold compared to the expression level in NIH3T3/4E cells in complete medium or NIH3T3 cells in serum replete media. To examine whether the mRNA levels changed accordingly, we measured the total mRNA levels in NIH 3T3 and NIH 3T3/4E cells when grown in replete media or serum starved (Figure 7C). There was no strict concordance between the protein and mRNA levels. For example, when NIH 3T3/4E cells were serum starved, osteopontin protein levels increased 6-fold compared

to serum replete levels, whereas mRNA abundance increased ~2-fold. Similarly, comparing NIH 3T3/4E cells to NIH 3T3 cells when both were in replete media, osteopontin protein level was similar, while mRNA levels differed 2- to 3-fold. These results indicate that posttranscriptional control is important for the expression of osteopontin.

We next examined the functional role of osteopontin in our model and utilized siRNAs to specifically reduce the levels in NIH 3T3/4E cells. Osteopontin (Spp1) siRNA#1 or osteopontin siRNA#2 (at 20 nM) decreased the levels of osteopontin protein in NIH 3T3/4E cells at 10% serum by ~30%, assessed by western blotting, and by ~60% by RNA levels (data not shown) compared to a scrambled osteopontin siRNA#1 (Spp1 siRNA#1-scrambled) (Figure 7C, lower panel). A functional assay using osteopontin siRNA#1 (or osteopontin siRNA#2) revealed a significant loss of apoptosis resistance in NIH 3T3/4E cells, with apoptosis reaching 11% at 20 nM siRNA concentration (Figure 7D; both siRNAs were equally efficient, data using one siRNA#1 and ostepontin siRNA#1-scrambled are shown). These results indicate that the set of gene products identified did contain transcripts subject to posttranscriptional control with important functions in apoptosis regulation, and that osteopontin is necessary for some of the apoptosis resistance observed in the NIH 3T3/4E model.

DISCUSSION

Posttranscriptional control is recognized to have a central role in normal and malignant cell growth and differentiation. Recent studies have elucidated critical apical steps linking normal and pathological extracellular growth and survival signals through their cognate receptors to signaling intermediates which converge on eIF4E, the mRNA cap-binding component of the protein synthesis initiation machinery. Although a number of investigations have deduced the identity of individual transcripts which are targets for translational activation and mediate aspects of the anti-apoptotic and neoplastic function of eIF4E—no systematic, functionally verified genome-wide examination of the repertoire of translationally activated transcripts has been reported. Using global profiling of mRNA as a function of translational efficiency, here we identify a set of 255 transcripts whose translation is selectively activated in the context of eIF4E rescue from apoptosis. Among the identified transcripts, a high frequency of some groups of transcripts with shared functions was apparent after manually curating the annotation. In this regard, about one-third of transcripts that were translationally activated in NIH 3T3/4E cells subjected to apoptogenic stimuli encoded proteins involved in transcriptional control, signal transduction, mitochondrial function and the translational machinery itself.

The translationally activated mRNAs we identified encode a diverse group of regulatory and structural proteins. In principle, our gene list should include those with known—or to be discovered—functions in mediating the potent and pleotropic ability of an activated translation initiation apparatus to regulate cell fate as well as other phenomena controlled by eIF4E. Based on recently published studies in murine hematopoetic malignancy models (17) and human breast cancer (8,16), taken together with an extensive literature in the field of developmental biology, it is now understood that the translation initiation apparatus functions as a master integrator of trophic extracellular signals—both physiological and pathological—mediating their morphogenic, survival and oncogenic function. To orchestrate the output of proteins with such profound and coordinated impact on cell function, we expect that the set of translationally activated mRNA would be biased towards those associated with regulatory functions. In this regard, we found a large number of transcripts for transcription factors and signaling intermediates. In accord with the trophic function of the initiation machinery, we also identified translational activation of mRNA encoding mitochondrial proteins, proteins functioning in intermediary metabolism and components of the translational machinery.

Regulatory elements residing in the 3′-UTR and 5′-UTR of mRNA have important roles in posttranscriptional control (30). In this report we show that none of the known mRNA elements (as collected in UTRsite) was associated with the efficiency of ribosome loading onto transcripts when cells were rescued from apoptosis by enforced activation of the translation initiation apparatus. However, a novel 5′ 55mer was found to be overrepresented among translationally activated transcripts, and was predicted to fold into a secondary structure. We further demonstrated that the 55mer was sufficient to translationally activate a reporter gene when cells overexpressing eIF4E were subjected to serum withdrawal and that genes carrying the consensus hairpin structure are enriched for apoptosis and proliferation related genes. This indicates that although we do not know the full nature of the differences in affinity of eIF4E towards different transcripts, at least some of the specificity during apoptosis rescue and other functions mediated by deregulated eIF4E may reside in the consensus hairpin structure we have discovered—and by inference, in other elements yet to be discovered. More importantly our results indicate that at least some of the effects of eIF4E are mediated by defined elements in genes with similar functions, as proposed by the posttranscriptional operon theory. Although we can not exclude that other mechanisms also contribute to the phenotypic effects of deregulated eIF4E, our results clearly indicate that RNA element mediated co-regulation contributes to the apoptosis resistance in our model.

Our results examining the translational activation and rescue function of osteopontin also lend further support to the pleotropic nature of survival signaling emanating from eIF4E. Osteopontin is a phosphorylated acidic glycoprotein involved in mediation of the inflammatory response and may have a role in tumor progression as well (36,37). Of note, knockdown diminished rescue of cells from apoptosis by eIF4E—but did not ablate it. Thus, our data begin to shed light on specific transcripts subject to posttranscriptional control that may subserve critical functions in mediating the physiological and pathological functions of the translation initiation apparatus. It also has the potential to provide insight into the properties of those messages most influenced by the translational activity state of the cell.

Although powerful, our experimental approach to global translational profiling is not without its limitations. Applying technology to biological systems that rapidly generate large datasets requires a high level of technical precision.

In addition, polyribosome analysis as a tool to assess translational activity may over- or under-represent transcripts translated in different subcellular niches, loci or organelles; may overestimate translational activity as a function of increasing transcript size; and may fail to accurately identify transcripts activated due to increased nuclear-cytoplasmic transport (38). Moreover, it is important to acknowledge that there may be indirect translational consequences of the strong physiological perturbations we impose. Despite these limitations, our findings now enable biological and biomedical scientists to systematically study the posttranscriptional control in a wide variety of biological systems and human diseases in an unbiased and reproducible manner and provide the potential of identifying novel mRNA regulatory elements that are involved in posttranscriptional control.

SUPPLEMENTARY DATA

Supplementary Data are available at NAR Online.

ACKNOWLEDGEMENTS

We thank Dr Wayne Xu from Computational Genetics Laboratory at the University of Minnesota for suggestions about the RNA regulatory element search and technical support of computers in Computational Genetics Laboratory. Funding sources include NIH 1K08-HL074058-01, NIH P01 AI50162, NIH P50 HL50152, NIH HL076779, NIH HL073719, NIH T32 HL07741 and the University of Minnesota Carlson Family Fund. O.L. is supported by a postdoctoral fellowship from the Swedish Research Council. Special thanks to E. Ljungstrom for invaluable assistance with method development. Funding to pay the Open Access publication charges for this article was provided by NIH.

Conflict of interest statement. None declared.

REFERENCES

1. Keene,J.D. and Lager,P.J. (2005) Post-transcriptional operons and regulons co-ordinating gene expression. *Chromosome Res.*, **13**, 327–337.
2. Dever,T.E. (2002) Gene-specific regulation by general translation factors. *Cell*, **108**, 545–556.
3. Preiss,T. and Hentze,M.W. (2003) Starting the protein synthesis machine: eukaryotic translation initiation. *Bioessays*, **25**, 1201–1211.
4. Hershey,J. and Merrick,W. (2000) The pathway and mechanism of protein synthesis. In Sonenberg,N., Hershey,J. and Mathews,M. (eds), *Translational Control of Gene Expression*. Cold Spring Harbor Laboratory Press, Cold Spring Harbor, NY, pp. 33–88.
5. Clark,I.E., Wyckoff,D. and Gavis,E.R. (2000) Synthesis of the posterior determinant Nanos is spatially restricted by a novel cotranslational regulatory mechanism. *Curr. Biol.*, **10**, 1311–1314.
6. Rosenwald,I.B., Chen,J.J., Wang,S., Savas,L., London,I.M. and Pullman,J. (1999) Upregulation of protein synthesis initiation factor eIF-4E is an early event during colon carcinogenesis. *Oncogene*, **18**, 2507–2517.
7. Seki,N., Takasu,T., Mandai,K., Nakata,M., Saeki,H., Heike,Y., Takata,I., Segawa,Y., Hanafusa,T. and Eguchi,K. (2002) Expression of eukaryotic initiation factor 4E in atypical adenomatous hyperplasia and adenocarcinoma of the human peripheral lung. *Clin. Cancer Res.*, **8**, 3046–3053.
8. Li,B.D., Gruner,J.S., Abreo,F., Johnson,L.W., Yu,H., Nawas,S., McDonald,J.C. and DeBenedetti,A. (2002) Prospective study of eukaryotic initiation factor 4E protein elevation and breast cancer outcome. *Ann. Surg.*, **235**, 732–738; discussion 738–739.
9. Braun-Dullaeus,R.C., Mann,M.J., Seay,U., Zhang,L., von Der Leyen,H.E., Morris,R.E. and Dzau,V.J. (2001) Cell cycle protein expression in vascular smooth muscle cells *in vitro* and *in vivo* is regulated through phosphatidylinositol 3-kinase and mammalian target of rapamycin. *Arterioscler. Thromb. Vasc. Biol.*, **21**, 1152–1158.
10. Gupta,M., Sueblinvong,V., Raman,J., Jeevanandam,V. and Gupta,M.P. (2003) Single-stranded DNA-binding proteins PURalpha and PURbeta bind to a purine-rich negative regulatory element of the alpha-myosin heavy chain gene and control transcriptional and translational regulation of the gene expression. Implications in the repression of alpha-myosin heavy chain during heart failure. *J. Biol. Chem.*, **278**, 44935–44948.
11. Jitrapakdee,S., Gong,Q., MacDonald,M.J. and Wallace,J.C. (1998) Regulation of rat pyruvate carboxylase gene expression by alternate promoters during development, in genetically obese rats and in insulin-secreting cells. Multiple transcripts with 5′-end heterogeneity modulate translation. *J. Biol. Chem.*, **273**, 34422–34428.
12. De Benedetti,A. and Harris,A.L. (1999) eIF4E expression in tumors: its possible role in progression of malignancies. *Int. J. Biochem. Cell Biol.*, **31**, 59–72.
13. Cohen,N., Sharma,M., Kentsis,A., Perez,J.M., Strudwick,S. and Borden,K.L. (2001) PML RING suppresses oncogenic transformation by reducing the affinity of eIF4E for mRNA. *EMBO J.*, **20**, 4547–4559.
14. Lazaris-Karatzas,A., Montine,K.S. and Sonenberg,N. (1990) Malignant transformation by a eukaryotic initiation factor subunit that binds to mRNA 5′ cap. *Nature*, **345**, 544–547.
15. Polunovsky,V.A., Rosenwald,I.B., Tan,A.T., White,J., Chiang,L., Sonenberg,N. and Bitterman,P.B. (1996) Translational control of programmed cell death: eukaryotic translation initiation factor 4E blocks apoptosis in growth-factor-restricted fibroblasts with physiologically expressed or deregulated Myc. *Mol. Cell. Biol.*, **16**, 6573–6581.
16. Avdulov,S., Li,S., Michalek,V., Burrichter,D., Peterson,M., Perlman,D.M., Manivel,J.C., Sonenberg,N., Yee,D., Bitterman,P.B. *et al.* (2004) Activation of translation complex eIF4F is essential for the genesis and maintenance of the malignant phenotype in human mammary epithelial cells. *Cancer Cell*, **5**, 553–563.
17. Wendel,H.G., De Stanchina,E., Fridman,J.S., Malina,A., Ray,S., Kogan,S., Cordon-Cardo,C., Pelletier,J. and Lowe,S.W. (2004) Survival signalling by Akt and eIF4E in oncogenesis and cancer therapy. *Nature*, **428**, 332–337.
18. Li,S., Takasu,T., Perlman,D.M., Peterson,M.S., Burrichter,D., Avdulov,S., Bitterman,P.B. and Polunovsky,V.A. (2003) Translation factor eIF4E rescues cells from Myc-dependent apoptosis by inhibiting cytochrome c release. *J. Biol. Chem.*, **278**, 3015–3022.
19. Gerber,A.P., Herschlag,D. and Brown,P.O. (2004) Extensive association of functionally and cytotopically related mRNAs with Puf family RNA-binding proteins in yeast. *PLoS Biol.*, **2**, E79.
20. Pesole,G., Liuni,S., Grillo,G., Licciulli,F., Mignone,F., Gissi,C. and Saccone,C. (2002) UTRdb and UTRsite: specialized databases of sequences and functional elements of 5′ and 3′ untranslated regions of eukaryotic mRNAs. Update 2002. *Nucleic Acids Res.*, **30**, 335–340.
21. Rousseau,D., Kaspar,R., Rosenwald,I., Gehrke,L. and Sonenberg,N. (1996) Translation initiation of ornithine decarboxylase and nucleocytoplasmic transport of cyclin D1 mRNA are increased in cells overexpressing eukaryotic initiation factor 4E. *Proc. Natl Acad. Sci. USA*, **93**, 1065–1070.
22. Grolleau,A., Bowman,J., Pradet-Balade,B., Puravs,E., Hanash,S., Garcia-Sanz,J.A. and Beretta,L. (2002) Global and specific translational control by rapamycin in T cells uncovered by microarrays and proteomics. *J. Biol. Chem.*, **277**, 22175–22184.
23. Preiss,T., Baron-Benhamou,J., Ansorge,W. and Hentze,M.W. (2003) Homodirectional changes in transcriptome composition and mRNA translation induced by rapamycin and heat shock. *Nature Struct. Biol.*, **10**, 1039–1047.
24. Tusher,V.G., Tibshirani,R. and Chu,G. (2001) Significance analysis of microarrays applied to the ionizing radiation response. *Proc. Natl Acad. Sci. USA*, **98**, 5116–5121.
25. Larsson,O., Wahlestedt,C. and Timmons,J.A. (2005) Considerations when using the significance analysis of microarrays (SAM) algorithm. *BMC Bioinformatics*, **6**, 129.

26. Larsson,O., Scheele,C., Liang,Z., Moll,J., Karlsson,C. and Wahlestedt,C. (2004) Kinetics of senescence-associated changes of gene expression in an epithelial, temperature-sensitive SV40 large T antigen model. *Cancer Res.*, **64**, 482–489.
27. Liu,X., Brutlag,D.L. and Liu,J.S. (2001) BioProspector: discovering conserved DNA motifs in upstream regulatory regions of co-expressed genes. *Pac. Symp. Biocomput.*, 127–138.
28. Jensen,S.T. and Liu,J.S. (2004) BioOptimizer: a Bayesian scoring function approach to motif discovery. *Bioinformatics*, **20**, 1557–1564.
29. Hosack,D.A., Dennis,G.,Jr, Sherman,B.T., Lane,H.C. and Lempicki,R.A. (2003) Identifying biological themes within lists of genes with EASE. *Genome Biol.*, **4**, R70.
30. Wilkie,G.S., Dickson,K.S. and Gray,N.K. (2003) Regulation of mRNA translation by 5′- and 3′-UTR-binding factors. *Trends Biochem. Sci.*, **28**, 182–188.
31. Culjkovic,B., Topisirovic,I., Skrabanek,L., Ruiz-Gutierrez,M. and Borden,K.L. (2005) eIF4E promotes nuclear export of cyclin D1 mRNAs via an element in the 3′UTR. *J. Cell Biol.*, **169**, 245–256.
32. Harris,M.A., Clark,J., Ireland,A., Lomax,J., Ashburner,M., Foulger,R., Eilbeck,K., Lewis,S., Marshall,B., Mungall,C. *et al.* (2004) The Gene Ontology (GO) database and informatics resource. *Nucleic Acids Res.*, **32**, D258–D261.
33. Ashburner,M., Ball,C.A., Blake,J.A., Botstein,D., Butler,H., Cherry,J.M., Davis,A.P., Dolinski,K., Dwight,S.S., Eppig,J.T. *et al.* (2000) Gene ontology: tool for the unification of biology. The Gene Ontology Consortium. *Nature Genet.*, **25**, 25–29.
34. Khan,S.A., Lopez-Chua,C.A., Zhang,J., Fisher,L.W., Sorensen,E.S. and Denhardt,D.T. (2002) Soluble osteopontin inhibits apoptosis of adherent endothelial cells deprived of growth factors. *J. Cell Biochem.*, **85**, 728–736.
35. Geissinger,E., Weisser,C., Fischer,P., Schartl,M. and Wellbrock,C. (2002) Autocrine stimulation by osteopontin contributes to antiapoptotic signalling of melanocytes in dermal collagen. *Cancer Res.*, **62**, 4820–4828.
36. Denhardt,D.T., Noda,M., O'Regan,A.W., Pavlin,D. and Berman,J.S. (2001) Osteopontin as a means to cope with environmental insults: regulation of inflammation, tissue remodeling, and cell survival. *J. Clin. Invest.*, **107**, 1055–1061.
37. Rittling,S.R. and Chambers,A.F. (2004) Role of osteopontin in tumour progression. *Br J. Cancer*, **90**, 1877–1881.
38. Topisirovic,I., Guzman,M.L., McConnell,M.J., Licht,J.D., Culjkovic,B., Neering,S.J., Jordan,C.T. and Borden,K.L. (2003) Aberrant eukaryotic translation initiation factor 4E-dependent mRNA transport impedes hematopoietic differentiation and contributes to leukemogenesis. *Mol. Cell. Biol.*, **23**, 8992–9002.